The influence of dissolved molecular oxygen on the corrosion of metals in aqueous acid solutions. Review*

Ya.G. Avdeev* and Yu.I. Kuznetsov

A.N. Frumkin Institute of Physical Chemistry and Electrochemistry, Russian Academy of Sciences, Leninsky pr. 31, 119071 Moscow, Russian Federation
**E-mail: avdeevavdeev@mail.ru*

Abstract

This review discusses the current state of research in the field of corrosion of metals in aqueous solutions of acids containing molecular oxygen, as well as various issues of inhibitory protection of metals in such acidic environments. Thermodynamic aspects of metal corrosion in aqueous media containing dissolved O_2 are discussed. Reference data on the physicochemical properties of O_2 present in acidic aqueous media is presented. Modern views on the mechanism of O_2 reduction on metals are discussed. Corrosion of a metal in such an acid solution containing O_2 generally occurs as a result of its parallel reactions of interaction with the acid itself and O_2 molecules. In the case of metals with $E^0(Me^{z+}/Me)>0$ V, the only possible reaction is interaction with O_2. A specific feature of corrosion occurring with oxygen depolarization is its diffusion control, which makes this process very sensitive to the nature of convection of the aggressive environment. An increase in the rate of corrosion of metals is caused by an increase in the O_2 content in the solution and the transition from a static environment to a dynamic one. The presence of molecular O_2 in acid solutions reduces the effectiveness of metal protection with corrosion inhibitors, in comparison with similar oxygen-free environments. In inhibited environments containing O_2, the sensitivity of metal corrosion to the parameters of solution convection remains. The bibliography includes 109 references.

Received: May 16, 2024. Published: June 6, 2024 doi: 10.17675/2305-6894-2024-13-2-25

Keywords: *corrosion, metal, mechanism of metal corrosion, acid corrosion, dissolved oxygen, oxygen reduction reaction, corrosion inhibitors.*

I. Introduction

Acid solutions used in real production processes often come into contact with air and as a result are saturated with dissolved molecular oxygen, which can lead to a change in their properties and aggressiveness towards metals in contact with them. The content of dissolved oxygen in these environments will be low, but at the same time it behaves as a strong oxidizing agent in the system. As a result, contact of the metal with such acidic environments

*This study was carried out as part of R&D (2022–2024): "Chemical resistance of materials, protection of metals and other materials from corrosion and oxidation" (EGISU registration number 122011300078-1, inventory number FFZS-2022-0013).

should potentially be accompanied by a corrosion process determined by two cathodic reactions – the reduction of protons and molecular oxygen. In addition, the low oxygen content in such corrosive environments will lead to the fact that the corrosion of metals occurring at the interface with the aqueous medium will occur with diffusion restrictions. In aqueous environments, processes occurring with diffusion restrictions are very sensitive to the hydrodynamic parameters of the liquid medium. It is logical to assume that the corrosion of metals in acid solutions containing O_2 can significantly depend on the flow rate of the aggressive medium.

Based on their ability to displace hydrogen gas from aqueous acid solutions, existing metals are divided into two groups. The first group consists of metals capable of displacing gaseous H_2 from acid solutions, for which the value of the standard redox potential of the Me^{z+}/Me pair ($E^0(Me^{z+}/Me)<0$ V. The second group consists of metals with $E^0(Me^{z+}/Me)>0$ V, which are incapable of displacing H_2. Potentially, metals of the first group will react with an acid solution containing molecular oxygen as a result of their oxidation by protons and O_2 molecules. In the case of metals of the second group, their corrosion in such environments (with the exception of metallic gold that is thermodynamically stable in them) – the result of oxidation with dissolved O_2. These patterns can be clearly demonstrated by analyzing the Pourbaix diagrams of the Fe–H_2O and Cu–H_2O systems [1, 2], in which a metal from the first and second groups is represented as a component.

In the Fe–H_2O system (Figure 1), for acid media, the lower limit of stability of water (line *a*) is located in the region of higher potentials than the stability limit of metallic Fe (line 1). Between these lines there is a region in which metallic Fe is thermodynamically unstable, but gaseous H_2 is stable. In this region the reaction is thermodynamically allowed:

$$Fe + 2H^+ = Fe^{2+} + H_2. \quad (I.1)$$

In parallel with this, between the stability limit of metallic Fe (line 1) and the upper limit of stability of water (line *b*) there is a region in which metallic Fe and gaseous O_2 are unstable. Therefore, the reaction is allowed:

$$2Fe + O_2 + 4H^+ = 2H_2O + 2Fe^{2+}. \quad (I.2)$$

Thus, in acid solutions containing dissolved O_2, reactions (I.1) and (I.2) are allowed during iron corrosion.

In addition, data from the *E*–pH diagram of the Fe–H_2O system make it possible to predict the possibility of an indirect effect of dissolved O_2 on the corrosion of metallic Fe in an acidic environment. The product of Fe corrosion in an acidic environment is Fe(II) cations. The upper limit of their stable existence (line 2) lies below the upper limit of water stability (line *b*). Between them there is a region where Fe(II) cations and molecular O_2 are unstable. The following process is allowed in this area:

$$4Fe^{2+} + O_2 + 4H^+ = 2H_2O + 4Fe^{3+}. \quad (I.3)$$

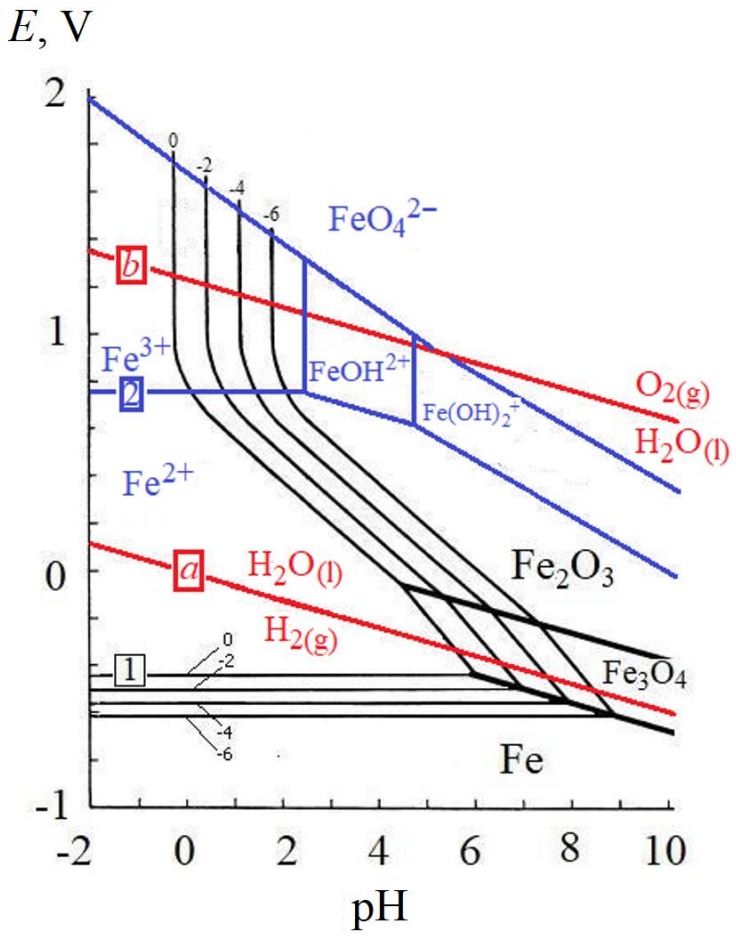

Figure 1. Fragment of the *E*–pH diagram of the stability fields of metallic iron in water at 25°C and 101.3 kPa total pressure. We consider only Fe, Fe_3O_4 and Fe_2O_3 to be solid phases [1]. Stability fields are given for cases where lg *a*(Fe(III) = lg *a*(Fe(II)) and corresponds to the values –6, –4, –2 and 0.
a – $2H^+ + 2e^- = H_{2(g)}$, $E = -(0.059/2)\lg p(H_2) - 0.059$ pH (low limits of stability of water);
b – $O_{2(g)} + 4H^+ + 4e^- = 2H_2O_{(l)}$, $E = 1.23 + (0.059/4)\lg p(O_2) - 0.059$ pH (high limits of stability of water);
1 – $Fe^{2+} + 2e^- = Fe$, $E = -0.440 + 0.0295 \lg a(Fe^{2+})$;
2 – $Fe^{3+} + e^- = Fe^{2+}$, $E = 0.771$.

As a result, an additional strong oxidizing agent, Fe^{3+} cations, appears in the corrosive environment. The oxidation of Fe^{3+} salts with atmospheric oxygen in acid solutions is discussed in [3–7].

According to the *E*–pH diagram of the Fe–H_2O system, the fields of stable existence in acidic environments of Fe(III) cations and metallic iron are spaced apart. Between them there is a region of their unstable existence, which determines the possibility of the following reaction occurring for the system under consideration:

$$2Fe^{3+} + Fe = 3Fe^{2+}. \quad (I.4)$$

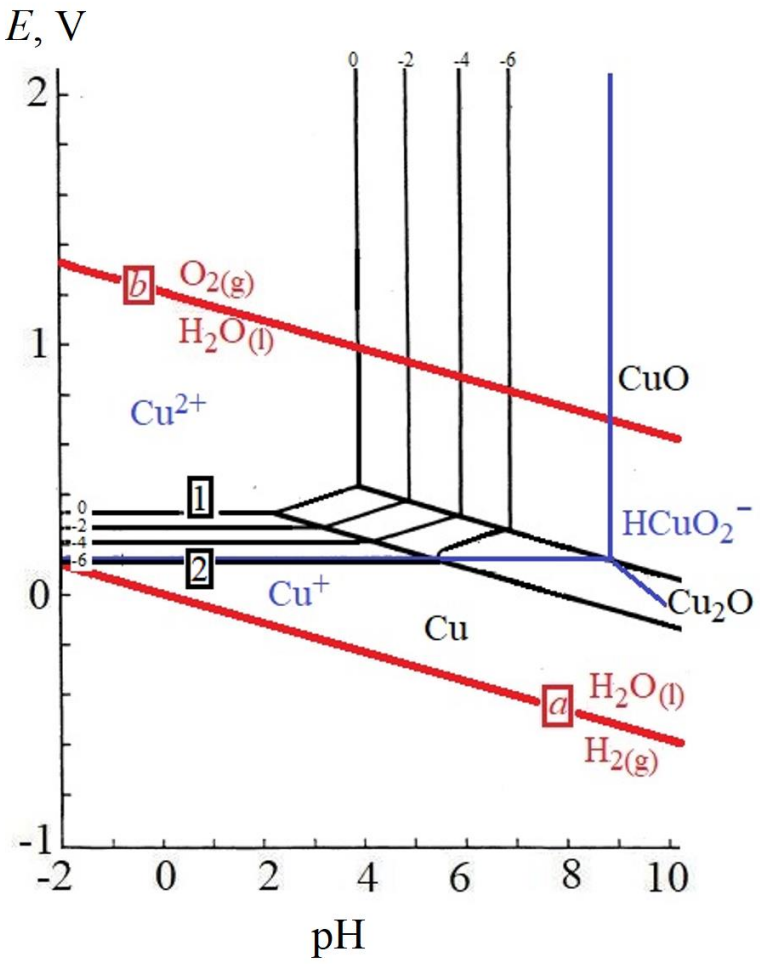

Figure 2. Fragment of the *E*–pH diagram of the stability fields of metallic copper in water at 25°C and 101.3 kPa total pressure. We consider only Cu, Cu_2O and CuO to be solid phases [2]. Stability fields are given for cases where lg *a*(Cu(II) corresponds to the values –6, –4, –2 and 0.

a – $2H^+ + 2e^- = H_{2(g)}$, $E = -(0.059/2)\lg p(H_2) - 0.059$ pH (low limits of stability of water);

b – $O_{2(g)} + 4H^+ + 4e^- = 2H_2O_{(l)}$, $E = 1.23 + (0.059/4)\lg p(O_2) - 0.059$ pH (high limits of stability of water);

1 – $Cu^{2+} + 2e^- = Cu$, $E = 0.337 + 0.0295 \lg a(Cu^{2+})$;

2 – $Cu^+ + e^- = Cu$, $E = 0.520 + 0.0591 \lg a(Cu^+)$, $\lg a(Cu^+) = -7$.

Analysis of the *E*–pH diagram of the Fe–H_2O system shows that in acid solutions containing molecular O_2, corrosion of iron can occur not only through reactions (I.1) and (I.2), but also through reaction (I.4). Features of corrosion of steels in acid solutions containing Fe(III) salts are discussed in works [8–10]. The reasons for the low efficiency of steel corrosion inhibitors in these environments have also been identified [8, 11, 12].

In the Cu–H_2O system (Figure 2), for acid media, the lower limit of stability of water (line *a*) is located in the region of lower potentials than the stability limit of metallic Cu (line 1). As a result, there is no region in the diagram in which metallic copper is unstable, but gaseous H_2 is stable. Displacement of hydrogen gas by copper from acid solutions will

not occur. However, between the stability limit of metallic Cu (lines 1 and 2) and the upper limit of stability of water (line *b*) there is a region in which metallic Cu and gaseous O_2 are unstable. Therefore, the following reactions are allowed:

$$2Cu + O_2 + 4H^+ = 2H_2O + 2Cu^{2+}, \quad (I.5)$$

$$4Cu + O_2 + 4H^+ = 2H_2O + 4Cu^+. \quad (I.6)$$

Thus, in acid solutions containing dissolved O_2, during copper corrosion, reactions (I.5) and (I.6) are possible, but copper cannot displace hydrogen from the acid.

The influence of molecular O_2 present in acid solutions on the corrosion of steels is not always clear. It can cause passivation of stainless steels in cold aerated solutions of H_2SO_4 [13, 14] and of iron in weakly acidic solutions of organic acids [15]. In the cases under consideration, molecular O_2 itself acts as a so-called "oxidative type" corrosion inhibitor.

There are a large number of recent studies [16–23] devoted to the consideration of various aspects of metal corrosion in acidic environments and their inhibitory protection. However, these studies did not address the issue of the influence of molecular O_2 on the corrosion of metals in acid solutions and the effectiveness of inhibitors used to slow down the corrosion of metals.

Based on the above, it seems important to summarize and systematize information about the corrosion of metals in acid solutions containing molecular O_2, and various aspects of the inhibitory protection of metals in such environments. Understanding the characteristics of metal corrosion in acid solutions containing dissolved O_2 is impossible without discussing related issues related to the consideration of some physicochemical properties of molecular O_2 and the mechanism of its cathodic reduction on metals.

II. Some Physicochemical Properties of Molecular Oxygen

II.1. Redox potential of O_2/H_2O pair

Dissolved O_2 in aqueous solutions is a strong oxidizing agent [24]. The overall process of O_2 reduction occurs with the participation of four electrons:

$$O_2 + 4H^+ + 4e^- = 2H_2O \text{ (acid media)}, \quad (II.1)$$

$$O_2 + 2H_2O + 4e^- = 4OH^- \text{ (alkaline media)}. \quad (II.2)$$

The value of the equilibrium potential corresponding to this reaction can be easily calculated using a thermodynamic approach from the value of the standard free energy of the formation of water from gaseous H_2 and O_2. At temperature $t = 25°C$ and oxygen pressure $p(O_2) = 101.3$ kPa, the value of this equilibrium potential is $E = 1.229$ V relative to the equilibrium potential of the hydrogen electrode in the same solution. Since the potentials of the equilibrium hydrogen and oxygen electrodes change equally with the pH of the solution, the difference in these potentials does not depend on the composition of the solution. If the potential is measured relative to the potential of a normal hydrogen electrode (in an acidic solution with pH = 0), then the equilibrium potential of the oxygen electrode, which shifts

negatively by 59 mV with an increase in pH by one unit, has the value $E = 0.401$ V in an alkaline solution with pH = 14. A characteristic feature of the oxygen electrode is that the value of the equilibrium potential calculated thermodynamically, as a rule, is not established experimentally. On inert electrodes, when immersed in an electrolyte and in contact with gaseous oxygen, a potential value between 0.8 and 1.1 V is established. The magnitude of the established potential depends on the pretreatment of the electrode.

II.2. Oxygen solubility in aqueous solutions

Works [25–30] discuss data on the solubility of molecular O_2 in water and aqueous solutions depending on temperature and pressure. Oxygen solubility in pure or fresh water at 25°C and 1.0 atm of O_2 pressure is about 1.22 mmol/L (the values are varied from 1.18 to 1.25 mmol/L as reported in review [30]). In air with a normal composition, the oxygen partial pressure is 0.21 atm, the O_2 solubility would become 0.256 mmol/L. The values of O_2 solubility in distilled water determined experimentally under these conditions are varied from 0.230 to 0.269 mmol/L as reported in [27].

The solubility of O_2 in acid solutions decreases with increasing their concentration (Table II.1). It also falls with increasing temperature, remaining lower for acid solutions than in pure water (Table II.2). It should be noted that increasing the temperature of water and H_2SO_4 solution by 100°C reduces the solubility of O_2 in them by 2.9 and 2.7 times.

Table II.1. Oxygen solubility in H_2SO_4 solutions. 25°C, 1.0 atm [30].

Parameter	***C*(H_2SO_4), M**							
	0	**0.05**	**0.10**	**0.50**	**1.00**	**2.00**	**3.00**	**4.00**
O_2 solubility, mmol/L	1.25	1.11	1.10	1.05	0.98	0.98	0.72	0.66

Table II.2. Oxygen solubility (mmol/L) at different temperatures and 1.0 atm pressure in water and H_2SO_4 solutions [30].

Water environment	**Temperature, °C**							
	0	**10**	**20**	**30**	**40**	**60**	**80**	**100**
Pure water	2.19	1.70	1.39	1.21	1.04	0.88	0.79	0.76
1 M H_2SO_4	1.77	1.41	1.17	0.99	0.87	0.72	0.67	0.65

Methods for studying O_2 solubility are summarized in [25]. In the study of the solubility of O_2 in liquids, methods are employed which are divided into physical, chemical, and physicochemical. The volumetric and manometric methods belong to the class of physical procedures. Their essential feature involves the measurement of the volume (pressure) of O_2 absorbed by the degassed liquid or desorbed from the liquid. Chemical methods are based on the interaction of O_2 with reductants. Among physicochemical methods, spectroscopic,

electrochemical, chromatographic, kinetic, radiometric, and mass-spectrometric methods as well as methods based on the paramagnetic properties of O_2 (EPR, NMR) are employed.

II.3. Oxygen diffusion coefficients in aqueous solutions

The estimation of oxygen diffusion coefficient $D(O_2)$ in aqueous solution could be conducted using the Stokes–Einstein equation using several known parameters such as the molecular weight of water, the absolute temperature, the solution viscosity, and the molar volume of water [30]. The mean experimental value of $D(O_2)$ in pure water is about $2 \cdot 10^{-5}$ cm^2 s^{-1} at 20°C. Experimental data for $D(O_2)$ in pure water at different temperatures were shown in Table II.3.

In acid solutions, the values of $D(O_2)$ are lower than in pure water [30]. In 0.1 M $HClO_4$, the value of $D(O_2)$ is $167 \cdot 10^{-7}$ cm^2 s^{-1} at 25°C; in 0.5 M H_2SO_4, the value of $D(O_2)$ is $140 \cdot 10^{-7}$ cm^2 s^{-1} at 25°C; in 14.6 M H_3PO_4, the value of $D(O_2)$ is $66.6 \cdot 10^{-7}$ cm^2 s^{-1} at 100°C and $82.9 \cdot 10^{-7}$ cm^2 s^{-1} at 120°C.

Table II.3. Oxygen diffusion coefficients in pure water at different temperatures and 1.0 atm O_2 pressure [30].

Parameter	Temperature, K						
	273	**288**	**293**	**298**	**308**	**318**	**333**
$D(O_2) \cdot 10^5$, cm^2 s^{-1}	1.2	1.5–1.7	2.0	1.9–2.3	2.6–2.9	3.4	4.0–4.6

II.4. Viscosity of aqueous solution

As will be discussed below, the O_2 reduction process on metals can occur with partial or complete diffusion control. The rate of such processes is regulated not only by the diffusion coefficient of the particles involved in them, but also by the viscosity of the medium in contact with the phase boundary where the chemical reaction takes place. The viscosity characteristics of water and aqueous solutions of acids are given in [30, 31]. The kinematic viscosity of water decreases with increasing temperature (Table II.4). Reference data on the relative viscosity of acid solutions is given in Table II.5.

Table II.4. Kinematic viscosity of pure liquid water at different temperatures and 1.0 atm pressure [30].

Parameter	Temperature, K								
	273	**278**	**283**	**293**	**303**	**313**	**333**	**353**	**373**
$\eta \cdot 10^2$, cm^2 s^{-1}	1.79	1.52	1.31	1.00	0.80	0.66	0.48	0.37	0.29

Table II.5. Relative viscosity of aqueous acid solutions at 25°C [31].

Acid	Equivalent concentration, M			
	0.125	**0.25**	**0.5**	**1.0**
HCl	1.0095	1.0166	1.0338	1.0671
$HClO_3$	1.0059	1.0145	1.0255	1.0520
$HClO_4$	0.9992	0.9998	1.0032	1.0118
H_2SO_4	1.0082	1.0216	1.0433	1.0898
H_3PO_4	1.0312	1.0656	1.1331	1.2871
H_3AsO_4	1.0309	1.0595	1.1291	1.2707
HNO_3	1.0027	1.0052	1.0115	1.0266
HBr	1.0068	1.0069	1.0164	1.0320
H_3CCOOH	1.0049	1.0092	1.0169	1.0312

III. Mechanism of Reduction of Molecular Oxygen on Metals

One of the earliest generalizations of ideas about the mechanism of O_2 reduction on metals was carried out in review [24]. Research in this area remains relevant to the present day [32–55]. Most often, studies of the kinetics of O_2 reduction are carried out on inert metals (Pt and Au). Important information about the kinetics of the O_2 reduction process can be obtained from current-voltage studies [51–55], chronopotentiometry [56, 57] and electrochemical impedance spectroscopy (EIS) [55]. Since this reaction can occur with diffusion limitations, electrochemical studies are often performed on rotating disk electrodes [35, 36, 55].

In acid solutions containing a strong oxidizing agent (molecular O_2), two additional cathodic partial processes are thermodynamically allowed [24] with the participation of four (Eq. II.1) and two (Eq. II.2) electrons. Based on an analysis of kinetic data, M.R. Tarasevich [55] proposed a scheme for the reduction of oxygen on metals in acid media (Figure 3). Similar schemes were discussed in [34, 39, 40, 42, 44–49]. For an inert gold electrode, the sequential reduction of oxygen is described as

$$O_{2(ads)} + e^- \leftrightarrow O^-_{2(ads)} \text{ or } O_{2(ads)} + H^+ + e^- \leftrightarrow HO_{2(ads)}, \quad \text{(III.1)}$$

$$O^-_{2(ads)} + e^- + 2H^+ \rightarrow H_2O_{2(ads)} \text{ or } HO_{2(ads)} + e^- + H^+ \rightarrow H_2O_{2(ads)}, \quad \text{(III.2)}$$

$$H_2O_{2(ads)} + e^- + H^+ \leftrightarrow H_2O + OH_{(ads)}, \quad \text{(III.3)}$$

$$OH_{(ads)} + e^- + H^+ \rightarrow H_2O, \quad \text{(III.4)}$$

including limiting stages (III.1) and (III.3) [55].

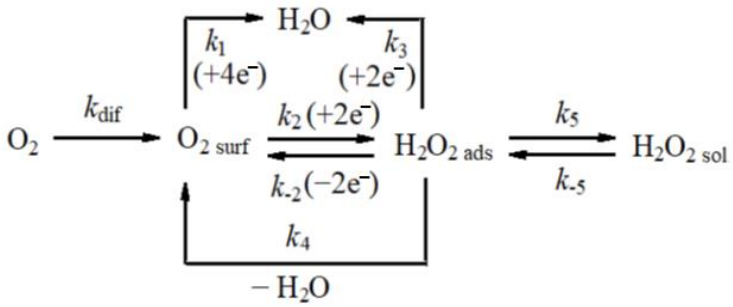

Figure 3. Possible reactions of oxygen reduction in an acidic medium: k_{dif} is the rate constant of oxygen diffusion from the bulk of the solution to the electrode's surface, k_1 is the rate constant of oxygen reduction along the four electron pathway, k_2 and k_3 are the constants of successive stages of oxygen reduction with the formation of an intermediate particle, k_{-2} is the rate constant of hydrogen peroxide oxidation, k_4 is the constant of the chemical decomposition of hydrogen peroxide, k_5 (k_{-5}) is the rate constant of the desorption (adsorption) of hydrogen peroxide on the electrode's surface [55].

It is noted [35, 39, 41, 42, 49, 58–61] that the rate of cathodic reduction of molecular O_2 depends on the hydrodynamic parameters of the medium, which is typical for processes with mixed kinetics or diffusion control. The diffusion current resulting from the reduction of O_2 on a metal rotating disk electrode in a laminar flow of liquid is described by the Levich equation:

$$i_d = 0.62zFC^*D^{2/3}\eta^{-1/6}n^{1/2}, \quad \text{(III.5)}$$

where z is the number of electrons participating in the reaction on the electrode, F is the Faraday number, C^* is the concentration of molecular O_2 in the depth of the solution, D is the coefficient of diffusion of O_2, η is the kinematic viscosity of the liquid, and n is the angular velocity of disk rotation.

Oxygen reduction reaction (ORR) was studied on polycrystalline Pt and Au electrodes in 0.1 M $HClO_4$ solutions containing various amounts of acetonitrile [61]. The state of the electrode surface was characterized by cyclic voltammetry in oxygen free electrolytes, while ORR studies were performed on Pt and Au rotating disc electrodes by a linear sweep voltammetry in oxygen saturated electrolytes. Acetonitrile is chemisorbed on Pt over a wide potential range. Initial potential of oxygen reduction is shifted negatively, while the kinetics of ORR is increasingly hindered with the increase of acetonitrile concentration. Inhibiting effect of acetonitrile on ORR is pronounced on both Pt and Au. Complete inhibition of ORR in the potential range of acetonitrile chemisorption is achieved for 0.1 M $HClO_4$ solution containing 1 M acetonitrile on Au and 3 M acetonitrile on Pt.

IV. Corrosion of Metals in Acid Solutions Containing Dissolved Molecular Oxygen

Elements of the electrochemical theory of metal corrosion are considered by L.I. Antropov in [62]. For electrochemical corrosion of metals to occur, it is required that the corrosive environment contain oxidizing particles that, under given conditions, can be reduced on the

surface of the metal, taking away electrons from it. For example, during corrosion of iron in a solution of sulfuric acid, protons act as such particles:

$$2H^+ + 2e^- = H_2, \quad \text{(IV.1)}$$

taking away electrons from iron:

$$Fe = Fe^{2+} + 2e^- \quad \text{(IV.2)}$$

and transferring it in solution in the form of aqua-cations. For reactions IV.1 and IV.2 to occur in the indicated direction, it is necessary that the equilibrium potential of iron ($_rE_{Me}$) be negative than the equilibrium potential of the hydrogen electrode ($_rE_H$):

$$_rE_{Me} - {}_rE_H < 0. \quad \text{(IV.3)}$$

According to the scheme of equations IV.1 and IV.2, corrosion proceeds with hydrogen depolarization; if dissolved molecular oxygen acts as an oxidizing agent, then corrosion proceeds with oxygen depolarization:

$$O_2 + 4H^+ + 4e^- = 2H_2O, \quad \text{(IV.4)}$$

$$2Fe = 2Fe^{2+} + 4e^-. \quad \text{(IV.5)}$$

Often processes of corrosion with hydrogen and oxygen depolarization are mutually superimposed, then corrosion with mixed or hydrogen-oxygen depolarization occurs.

In addition to H^+ and O_2, other oxidizing agents can act as depolarizers – high-valent ions of the corroding metal, for example:

$$Fe^{3+} + e^- = Fe^{2+} \quad \text{(IV.6)}$$

or ions of another metal, more electropositive than corrosive:

$$Cu^{2+} + 2e^- = Cu. \quad \text{(IV.7)}$$

Equation IV.6 corresponds to corrosion with oxidative depolarization, and IV.7 – with metallic depolarization. The condition for the thermodynamic occurrence of corrosion in all these cases is compliance with the inequality, which is a generalization of equation IV.3:

$$_rE_{Me} - {}_rE_{Ox} < 0, \quad \text{(IV.8)}$$

where $_rE_{Ox}$ is the equilibrium potential of the oxidizer. Equation IV.8 is a thermodynamic criterion for the possibility of an electrochemical reaction.

In all cases, two different reactions are combined at the electrode. As a consequence, the potential of the corroding metal (E_{cor}) cannot coincide with the equilibrium potential of either of them. When a stationary state is reached, the E_{cor} of the metal takes on a certain value that practically does not change over time. Such constancy of E_{cor} indicates the achievement of a charge balance, ensured by the fact that charges pass across the metal-corrosion medium interface in two opposite directions in equivalent quantities. The equilibrium potential $_rE$ also corresponds to a charge balance, and charge transfer is associated with the reduction and oxidation of the same particles. For example, for electrodes

of the 1st type – an ion (atom) of the metal of the electrode. He also receives the same reaction directly:

$$Me^{2+} + 2e^- = Me \quad \text{(IV.9)}$$

and reverse directions:

$$Me = Me^{2+} + 2e^-. \quad \text{(IV.10)}$$

At a stationary corrosion potential, at least two types of particles of equal nature or, more precisely, two different electrode reactions proceeding in mutually opposite directions participate in establishing the balance of charges. If the intensity of charge transfer is related to a unit of interface surface and a unit of time, then it can be characterized through the current density. In equilibrium at $E = {}_rE$,

$$i_{Me}^{\rightarrow} = i_{Me}^{\leftarrow} = i_{Me}^{0}. \quad \text{(IV.11)}$$

In the case where $E = E_{cor}$,

$$i_{Me}^{\rightarrow} + i_{Ox}^{\rightarrow} = i_{Me}^{\leftarrow} + i_{Ox}^{\leftarrow}. \quad \text{(IV.12)}$$

The corrosion density in current units i_{cor} corresponds to the difference in current densities in the reverse and forward directions for the metal (*i.e.*, the difference in the rates of the anodic ($i_{Me}^{\leftarrow}$) and cathodic ($i_{Me}^{\rightarrow}$) reactions for the metal) and, at the same time, the difference in current densities in the forward direction and in the opposite direction for the oxidizer (*i.e.*, the difference in the rates of the cathodic ($i_{Ox}^{\rightarrow}$) and anodic ($i_{Ox}^{\leftarrow}$) reactions):

$$i_{Me}^{\leftarrow} - i_{Me}^{\rightarrow} = i_{Ox}^{\rightarrow} - i_{Ox}^{\leftarrow} = i_{cor}. \quad \text{(IV.13)}$$

For corrosion with hydrogen depolarization, instead of V.13, we can write:

$$i_{Me}^{\leftarrow} - i_{Me}^{\rightarrow} = i_{H}^{\rightarrow} - i_{H}^{\leftarrow} = i_{cor}. \quad \text{(IV.14)}$$

The stationary corrosion potential E_{cor} is located between the equilibrium potentials ${}_rE_{Me}$ and ${}_rE_{Ox}$, and it is always more positive than ${}_rE_{Me}$ and negative than ${}_rE_{Ox}$. If this difference is large enough, then for a reaction involving a metal the cathodic process (discharge of metal ions, $i_{Me}^{\rightarrow}$) can be neglected, and for a reaction involving a depolarizer, the anodic process ($i_{Ox}^{\leftarrow}$) can be neglected. Then equations IV.13 and IV.14 are transformed:

$$i_{Me}^{\leftarrow} \approx i_{Ox}^{\rightarrow} \cong i_{cor}, \quad \text{(IV.15)}$$

$$i_{Me}^{\leftarrow} \approx i_{H}^{\rightarrow} \cong i_{cor}. \quad \text{(IV.16)}$$

During corrosion of metals with hydrogen depolarization, the rate of partial reactions of proton reduction and metal dissolution is limited by kinetic restrictions, most often by slowing down charge transfer, i.e. electrochemical overvoltage (Figure 4).

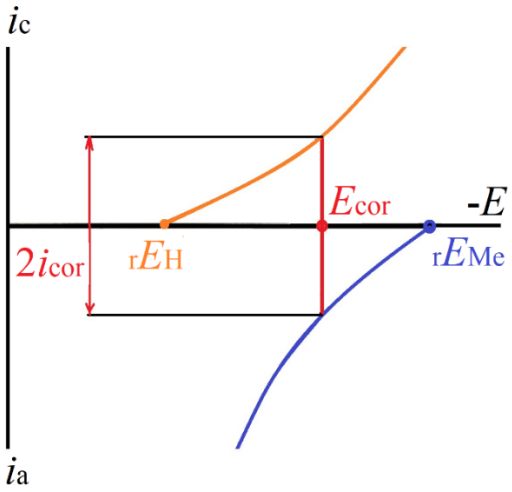

Figure 4. Polarization diagram of electrochemical corrosion with hydrogen depolarization.

In corrosion with oxygen depolarization, one of two partial reactions, namely the reduction of dissolved O_2, is usually realized with diffusion restrictions, at a limiting current that does not depend on the potential:

$$i(O_2) = i_{lim}(O_2) = D(O_2)C(O_2)\delta^{-1}, \quad \text{(IV.17)}$$

where $D(O_2)$ is the diffusion coefficient of O_2 in solution, $C(O_2)$ is the concentration of O_2 in solution, δ is the thickness of the diffusion layer in which the concentration gradient is concentrated. The corrosion rate is determined by the equation:

$$i^{\rightarrow}(O_2) = i^{\leftarrow}_{Me} = i_{lim}(O_2) = i_{cor}, \quad \text{(IV.18)}$$

which is illustrated in Figure 5. If the equilibrium potential of the metal and oxygen are close to each other and the intersection of the polarization curves occurs in the region of kinetic restrictions on oxygen, then instead of equation IV.18 the equation should be used:

$$i^{\rightarrow}(O_2) = i^{\leftarrow}_{Me} = i_{cor}. \quad \text{(IV.19)}$$

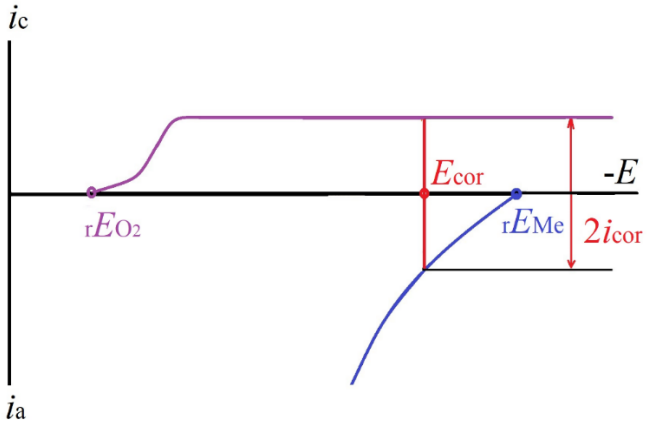

Figure 5. Polarization diagram of electrochemical corrosion with oxygen depolarization (kinetic limitations of the anodic reaction, diffusion limitations of the cathodic reaction).

The magnitude of the limiting diffusion current is determined by the geometry of the system in which corrosion occurs and by the speed of fluid movement. In the case of corrosion of thin plates onto which liquid flows at a speed v_0,

$$i_{lim}(O_2) = i_{cor} = 4FD^{1/3}\eta^{-1/6}x^{-1/6}v_0^{1/2}C(O_2), \quad \text{(IV.20)}$$

where x is the distance along the plate from the point where the liquid flows onto it. In the case of corrosion of a rotating metal disk, the equation simplifies to equation III.5.

In the case when the equilibrium potential of the metal is more negative than the potential of not only the oxygen, but also the hydrogen electrode, the metal corrodes as a result of two parallel processes of reduction of O_2 and H^+:

$$i_H^{\rightarrow} + i^{\rightarrow}(O_2) = i_{Me}^{\leftarrow} \equiv i_{cor} \quad \text{(IV.21)}$$

which is illustrated in Figure 6.

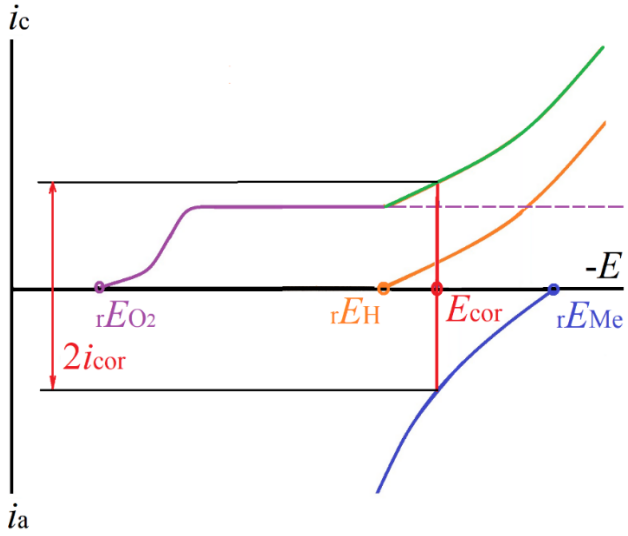

Figure 6. Polarization diagram of electrochemical corrosion with oxygen depolarization (kinetic limitations of the anodic reaction, mixed limitations of the cathodic reaction).

With an increase in the speed of movement of the corrosive medium, the value of $i_{lim}(O_2)$ according to equations IV.20 and III.5 will increase. This will lead to an acceleration of corrosion and an increase in the proportion of oxygen depolarization in it, since the rate of hydrogen evolution is limited by the stage of charge transfer, which is practically independent of the intensity of movement of the medium.

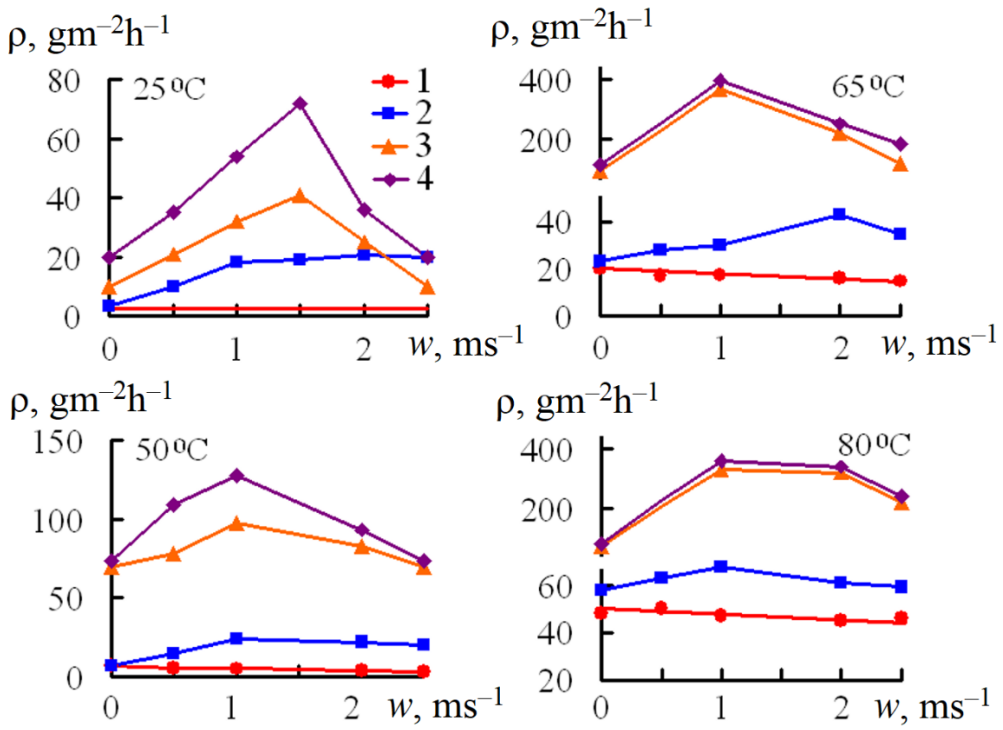

Figure 7. Influence of the flow velocity of an aggressive medium (*w*) on the corrosion rate of St1 steel (ρ) in 4% HCl (25–80°C) deaerated with hydrogen (1, 3) and aerated with oxygen (2, 4). Steel samples without (1, 2) and with thermal scale (3, 4). The scale-coated steel formed in air at 640°C.

The effect of dissolved O_2 on the corrosion of St1 low carbon steel coated with thermal scale in 4% HCl was studied depending on the flow rate of the corrosive medium and temperature [63]. It was shown that in 4% HCl deaerated with hydrogen, the corrosion rate of St1 steel increases with increasing temperature (Figure 7). Under these conditions, the acceleration of the circulation of the HCl solution somewhat reduces the value of the steel corrosion rate (ρ), which is believed to be a consequence of the slowing down of the hydrogen gas generation step. Hydrogen bubbles are more quickly washed from the metal surface and the solution is supersaturated with molecular hydrogen. In solutions saturated with molecular O_2, the *k* value of steel is higher than in deaerated media and depends on the flow velocity (*w*). The extreme nature of the dependence ρ–*w* is due to the fact that with an increase in the circulation rate of the medium, especially in heated media (50–80°C), where the solubility of oxygen is low, the effect of the flow on hydrogen depolarization is stronger than the stimulating effect of dissolved O_2. Corrosion of steel under scale occurs faster than in the same conditions in its absence. Accelerating the circulation of the solution first increases corrosion, and then reduces it. The effect of a decrease ρ value of steel at high *w* can be due to the washing out of Fe(III) cations, which are formed during the dissolution of scale and are capable of oxidizing the metal, from the near-electrode space into the bulk of the solution.

Potentiometry and voltammetry with a rotating disk electrode are used to study the corrosion of St3 low carbon steel in 1 M HCl (25°C) containing dissolved molecular oxygen from the mass loss of metal samples in a static and dynamic aggressive environment. It is shown that molecular oxygen in the acid solution and the transition from the static to dynamic state of an aggressive medium accelerates the corrosion of steel [64]. The corrosion of steel in this environment includes the anodic ionization of steel in the kinetic region and two partial cathodic reactions: the evolution of hydrogen and the reduction of dissolved molecular oxygen, characterized by kinetic and diffusion controls, respectively. Modeling the effect the hydrodynamic mode of the motion of a corrosive medium has on the rate of the cathodic reduction of molecular O_2 on steel using the equation III.5 and comparing the results to experimental data suggests with high probability that in the flow of a corrosive medium it mainly proceeds according to the scheme

$$O_2 + 2H^+ + 2e^- = H_2O_2. \qquad \text{(IV.22)}$$

The values of the true kinetic currents of the cathodic reaction are estimated for a steel disk electrode in 1 M HCl that is freely aerated with air and forcibly aerated with gaseous O_2. The effective coefficient of diffusion of dissolved molecular O_2 in 1 M HCl is established.

Some aspects of the electrochemical behavior of iron and carbon steel in aerated weakly acidic perchlorate and sulfate solutions are discussed in [65, 66].

The mechanism of the ORR on copper in a naturally aerated stagnant 0.5 M H_2SO_4 was studied using electrochemical methods [67]. The cathodic polarization curve showed three different regions. The three regions include a limiting current density region with the main transfer of $4e^-$ controlled by diffusion (–0.50…–0.40 V), a combined kinetic-diffusion region (–0.40…–0.20 V) with an additional $2e^-$ transfer due to the adsorption of the anions, and a hump phenomenon region (–0.20…–0.05 V), in which the chemical redox between the anodic intermediate and the cathodic intermediate, together with the electrochemical reaction, synergistically results in the acceleration of the ORR.

During corrosion of nickel in H_2SO_4 solutions containing O_2, its reduction occurs as a result of parallel reactions II.1 and IV.22 [68]. Hydrogen peroxide formed in reaction IV.22 can be reduced on a metal surface to H_2O, decompose to release O_2, and diffuse into the bulk of the acid solution. On a disk electrode, when it rotates intensively, the proportion of H_2O_2 formed can reach 25% of the theoretically possible.

In 2–5 M $HClO_4$ in the presence of oxygen, the true corrosion rate of copper, determined by measuring the mass loss of metal samples, exceeds the calculated values obtained during electrochemical studies by 3–5 times [69]. An autocatalytic effect is observed, caused by the accumulation over time in the solution of corrosion products – Cu(II) cations, which accelerate the destruction of the metal. It is assumed that copper corrosion in this environment occurs primarily through a catalytic mechanism in which copper dissolution predominantly occurs as a result of conjugate anodic

$$Cu = Cu^+ + e^-, \qquad \text{(IV.23)}$$

and cathodic reactions

$$Cu^{2+} + e^{-} = Cu^{+}. \quad \text{(IV.24)}$$

The concentration of the oxidizing agent (Cu(II) cations) is restored in a corrosive environment by chemical oxidation of Cu(I) cations with dissolved O_2. A similar picture is observed during corrosion of iron in 20% acetic acid in the presence of O_2, which also occurs *via* a catalytic mechanism through reactions IV.2 and IV.6. Fe(III) cations are formed in a corrosive environment during the oxidation of Fe(II) cations by molecular O_2. It should be noted that the patterns of corrosion of metals that form ions of different valences in acid solutions containing O_2 can differ significantly from the usual electrochemical mechanism.

Experimental data on the effect of dissolved O_2 on the corrosion of iron, carbon steel and nickel in H_2SO_4 solutions are presented in [70–72]. Data on the effect of dissolved O_2 on the corrosion of steel, Al, Pb, Cu, Ni, Sn and a number of alloys in solutions of H_2SO_4, HCl, HNO_3 and acetic acid are analyzed [73]. The experimental technique consisted of comparing corrosion rates in two solutions, one of which was saturated with oxygen and the other with hydrogen. The effects of velocity on the corrosion of copper in solutions of H_2SO_4, HCl and acetic acid has been studied. An apparatus in which the samples are suspended in the acid solution from a horizontal rotating wheel was used, and provision was made for air saturation or for total exclusion of O_2. The results emphasize the importance of O_2 in corrosion by dilute "nonoxidizing" acids.

Measurements of mass loss from disc made of β′-brass during corrosion in air saturated 1.0 M HCl at 30–60°C have been carried out [74]. At 30 and 40°C dissolution of β′-brass occurs in the activation regime. At 50°C the mixed-kinetics regime is observed while at 60°C the reaction is controlled diffusionally by the oxygen dissolved in the acid. At 30 and 40°C the main corrosion reactions are dissolution with oxygen depolarization and autocatalytic dissolution. At 60°C the autocatalytic dissolution disappears.

The corrosion behavior of tinplate in 0.1 M citric acid solution in aerated and deaerated conditions, respectively, were studied by a combination of EIS, inductively coupled plasma (ICP) and scanning electron microscopy (SEM). Under aerated conditions, three stages were distinguished during the corrosion process: the corrosion of tin coating, the corrosion of the carbon steel and the detachment of the surface corrosion product. Under deaerated conditions, the corrosion process of tinplate was dominated by the anodic dissolution of the tin coating [75].

V. Inhibitory Protection of Metals in Acid Solutions Containing Dissolved Molecular Oxygen

According to L.I. Antropov [62] during metal corrosion with hydrogen depolarization, in the case of additional superposition of oxygen depolarization (corrosion with mixed depolarization), the inhibition coefficient reflects the inhibition by the inhibitor of two cathodic reactions – hydrogen evolution and oxygen reduction:

$$\gamma = (\vec{i_H} + i(O_2))(\vec{i_{in,H}} + i_{in}(O_2))^{-1}, \quad (V.1)$$

where $\vec{i_H}$ and $i(O_2)$ are the current densities of the reduction of H^+ and molecular O_2 on the metal in a medium without an inhibitor, $\vec{i_H}$ and $i_{in}(O_2)$ are the current densities of the reduction of H^+ and molecular O_2 on the metal in a medium with the addition of an inhibitor. Typically, under corrosion conditions, the evolution of hydrogen is limited by kinetic limitations, and the reduction of O_2 by diffusion. In the presence of individual adsorption inhibitors, more effective suppression of hydrogen evolution ($\vec{i_H}$) occurs. Therefore, many inhibitors are less effective under conditions of mixed depolarization than during corrosion with pure hydrogen depolarization.

The selective effect of adsorption inhibitors on hydrogen depolarization is illustrated in Figure 8. Regardless of which reaction – cathodic or anodic – is affected by the inhibitor, the decrease in the overall corrosion rate or the rate of O_2 reduction is less noticeable than the decrease in the rate of hydrogen evolution. The action of adsorption inhibitors is characterized by a decrease in the overall corrosion rate with a simultaneous increase in the proportion of oxygen depolarization.

In the case of cathodic reduction of oxygen in the presence of inhibitors for some metals (Fe, Pt and Cu), regardless of the chemical nature of the additive, there is a noticeable decrease in the limiting current of O_2 reduction (Table V.1). This is explained by a decrease in the surface concentration of hydrogen and oxygen atoms caused by shielding of the metal surface by adsorbed particles. There is a decrease in the rate of oxygen reduction reaction, which becomes comparable to the rate of its diffusion. Under these conditions, the rate of the O_2 reduction process begins to be controlled by mixed kinetics, determined by the slowness of diffusion and the chemical reaction of hydrogen reduction (Figure 9). This conclusion is indicated by the deviation of the $i_d(O_2) - n^{1/2}$ dependence from linear in the presence of inhibitors. It is caused by the imposition of restrictions on diffusion associated with inhibition of the chemical reaction [76].

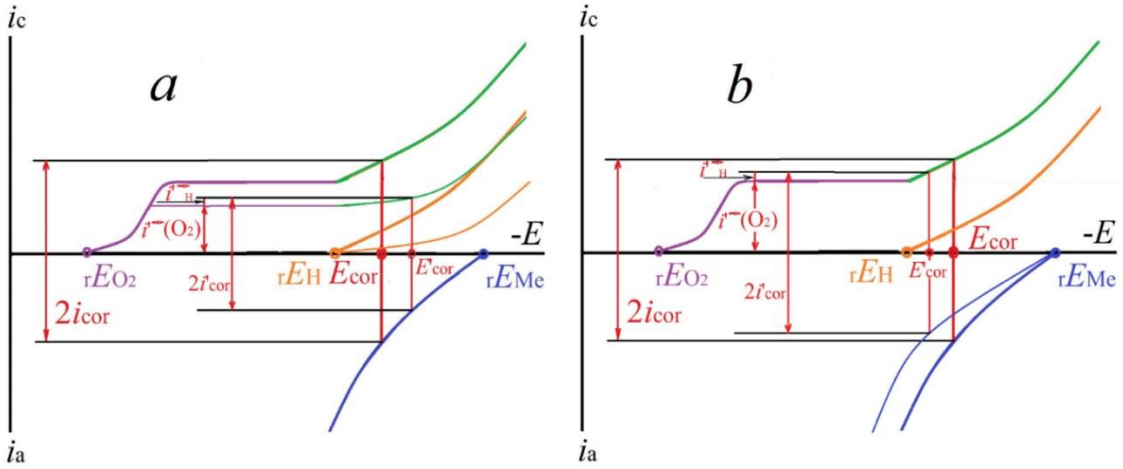

Figure 8. Polarization diagrams of the decrease of corrosion rate and the proportion of hydrogen depolarization under the action of a cathodic (*a*) and anodic (*b*) inhibitor.

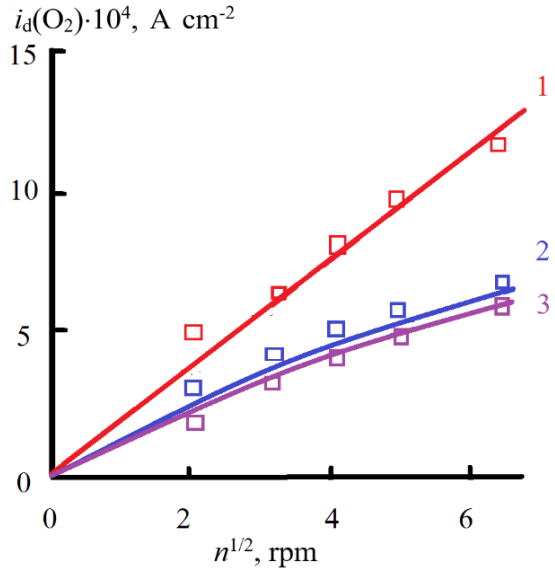

Figure 9. Effect of the rotation speed of an Armco iron disk in O_2 saturated 1 M H_2SO_4 (1), on the value of $i_d(O_2)$ in the presence of 10 mM dimethylolthiourea (2) and 10 mM inhibitor KPI-1 (3).

Table V.1. The influence of surfactants on the value of the limiting current of oxygen reduction ($i_d(O_2)\cdot10^4$, $A\cdot cm^{-2}$) on rotating metal disks (1000 rpm) in 1 N H_2SO_4 (room *t*).

Atmosphere above the solution	Fe	Pt	Cu	Cd	Cu(Hg)
Without additive					
Air	7.8	2.5	7.6	8.8	8.3
Oxygen	32	–	32	36	35
10 mM Decyl-3-hydroxypyridinium chloride					
Air	4.5	0.0	7.1	8.8	8.3
Oxygen	22	–	31	36	–
10 mM Monomethylolthiourea					
Air	4.7	0.0	–	8.9	8.2
Oxygen	22	–	–	36	–
10 mM Dimethylolthiourea					
Air	4.7	0.0	–	–	8.0
Oxygen	–	–	16	–	–

Table V.2. The effect of oxygen on the corrosion of steel 10 in 1 M HCl (room *t*, 8 h) in the presence of additives.

Additive	H_2 atmosphere		O_2 atmosphere	
	ρ, $g \cdot m^{-2} \cdot h^{-1}$	*Z*, %	ρ, $g \cdot m^{-2} \cdot h^{-1}$	*Z*, %
Without additive	1.2	–	0.81	–
0.3% I-1-A	0.044	96	0.27	67
0.3% Catapine K	0.11	91	0.27	67
0.3% Propargyl alcohol	0.12	90	0.24	70

In [77], the effect of dissolved O_2 on the corrosion of steel 10 in 1 M HCl (room *t*, 8 h) was studied. It was shown that in 1 M HCl in an atmosphere saturated with O_2, steel corrosion was slowed down in comparison with an environment saturated with H_2 (Table V.2). The resulting effect is associated with O_2 retardation of the dissolution of air-formed surface oxides present on the metal surface and protecting it from the action of acid. The presence of O_2 in a corrosive environment increases the proportion of sludge formed as a result of the dissolution of steel. In an environment saturated with O_2, it is 3.9% by weight. dissolved metal, in an environment saturated with H_2 – only 2.8%. In addition, in a solution saturated with O_2, the proportion of Fe(III) cations from the total content of Fe(II) and Fe(III) cations in a corrosive environment is 67%. In an environment without O_2, the proportion of Fe(III) cations is 0.8%. The presence of dissolved O_2 in the corrosive environment significantly reduced the protective effect of the studied corrosion inhibitors.

The effect of dissolved O_2 on the corrosion of steel 20 in an HCl solution (pH = 2.8, $t = 100$°C) with the addition of 30 mg/L N_2H_4 was studied under conditions of a flow of a corrosive medium (1 m/s). Corrosion of steel in such systems is accelerated by the presence of dissolved O_2, as well as the transition from a static to a dynamic environment (Table V.3) [78].

Table V.3. The corrosion rate of steel 20 (ρ, $g \cdot m^{-2} \cdot h^{-1}$) in aerated HCl solutions.

Hydrodynamics of the medium	N_2 atmosphere		Air atmosphere		O_2 atmosphere	
	Without N_2H_4	With N_2H_4	Without N_2H_4	With N_2H_4	Without N_2H_4	With N_2H_4
Static liquid	3.4	1.6	3.8	1.8	4.3	11
Fluid flow	5.1	3.5	7.1	6.0	8.3	17

It was shown the stimulating effect of dissolved O_2 on the corrosion of EI 448 steel in 10% HCl containing 0.5% catapin K [79]. The accelerating effect of O_2 on the corrosion of steel is more pronounced in the flow of a liquid medium (Table V.4).

The corrosion of St3 low-carbon steel in 1 M HCl (25°C) solution containing dissolved molecular oxygen with inhibition by butynediol and propargyl alcohol was studied by the voltammetric method using a disk electrode rotating at various velocities [80]. The corrosion of steel in the media under study is driven by three partial reactions: anodic ionization of iron and cathodic reduction of protons and molecular oxygen. The first two reactions occur in kinetic mode, while the latter reaction occurs in diffusion mode. An increase in the content of molecular oxygen in the acid solution, both in the presence and the absence of the inhibitors under study, accelerates steel corrosion due to acceleration of the cathodic reaction on the metal by oxygen. It is noted that dissolved oxygen reduces the efficiency of steel protection in HCl solutions by the corrosion inhibitors under study because they weakly hinder the cathodic reduction which occurs in diffusion mode.

There is a difference in the electrical double layer (EDL) capacity of Armco iron in inhibited 1 M HCl ($t = 18$°C) for H_2 deaerated and O_2 aerated environments (Table V.5). Higher values of the electrode capacity in environments aerated with O_2 are explained by the adsorption displacement of the inhibitor from the metal surface [81]. An increase in the EDL capacity of Armco iron in 1 M HCl containing propargyl alcohol is observed when O_2 gas is bubbled into the solution. Subsequent bubbling of H_2 gas into the solution, on the contrary, reduces the capacity of the EDL electrode. The observed effect is explained by the competitive adsorption of molecular oxygen and an organic inhibitor on iron [80].

Table V.4. The corrosion rate of EI 448 steel (ρ, $g \cdot m^{-2} \cdot h^{-1}$) in 10% HCl.

Additive	20°C	40°C	60°C	80°C
Static liquid				
Without additive	0.8	5.3	17	100
Catapine K	0.3	0.6	0.7	1.0
Without additive*	3.6	8.0	19	107
Catapine K*	2.2	2.6	7.6	8.0
Fluid Flow Rate – 1 $m \cdot s^{-1}$				
Without additive	3.1	8.0	20	23
Catapine K	1.2	1.9	4.2	5.2
Without additive*	4.5	21	33	58
Catapine K*	3.3	7.2	12	22
Fluid Flow Rate – 2 $m \cdot s^{-1}$				
Without additive	3.4	9.3	30	31
Catapine K	1.2	2.7	4.2	5.8
Without additive*	10	22	35	94
Catapine K*	3.5	6.6	15	19

Additive	20°C	40°C	60°C	80°C
Fluid Flow Rate – 3 m·s^{-1}				
Without additive	4.1	12	38	41
Catapine K	1.2	3.0	4.0	7.0
Without additive*	14	19	39	98
Catapine K*	5.6	7.7	12	23

* Bubbling oxygen gas into solution

Table V.5. Differential capacity of the double electrical layer of Armco iron ($S = 0.46$ cm^2) in 1 M HCl.

Additive	Differential capacitance of double electrical layer, μF	
	H_2 atmosphere	O_2 atmosphere
Without additive	9.41	15.1
0.1% Catapine A	2.00	5.52
0.03% Propargyl alcohol	3.91	8.68

Corrosion of carbon steel in HCl and Na_2SO_4 solution mixture was investigated using rotating cylinder electrode for a range of rotation velocity, 0–2000 rpm, solution temperature of 32–52°C, and different oxygen concentrations [82]. It is found that increasing O_2 concentration leads to a considerable increase in the corrosion rates especially at high rotational velocity. Indole and cetyl trimethyl ammonium bromides (CTAB) inhibitors exhibited very good inhibition efficiency in most conditions investigated with the former exhibited better inhibition efficiency arriving up to 87% at low rotational velocities. The inhibition efficiency of both inhibitors was found to decrease with increasing velocity. In addition, indole inhibitor reveals excellent inhibition efficiency even at high temperatures while CTAB efficiency decreased appreciably with temperature increase. The inhibiting action of six organic phosphonium compounds of the structure $[Ph_3P^+Y]X$, (Ph = phenyl, X = Br or Cl; and Y = propyl, propargyl, cyclopropyl, allyl, 1,3-dioxolanyl and cinnamyl), on the corrosion of mild steel in aerated 1 M HCl and 0.5 M H_2SO_4 (30°C) was studied using potentiodynamic and EIS techniques [83]. At the same time, the issue of the influence of dissolved O_2 on steel corrosion in the considered environments is left without discussion. The acceleration of corrosion of soft steels in inhibited acid solutions was noted in the works [84, 85].

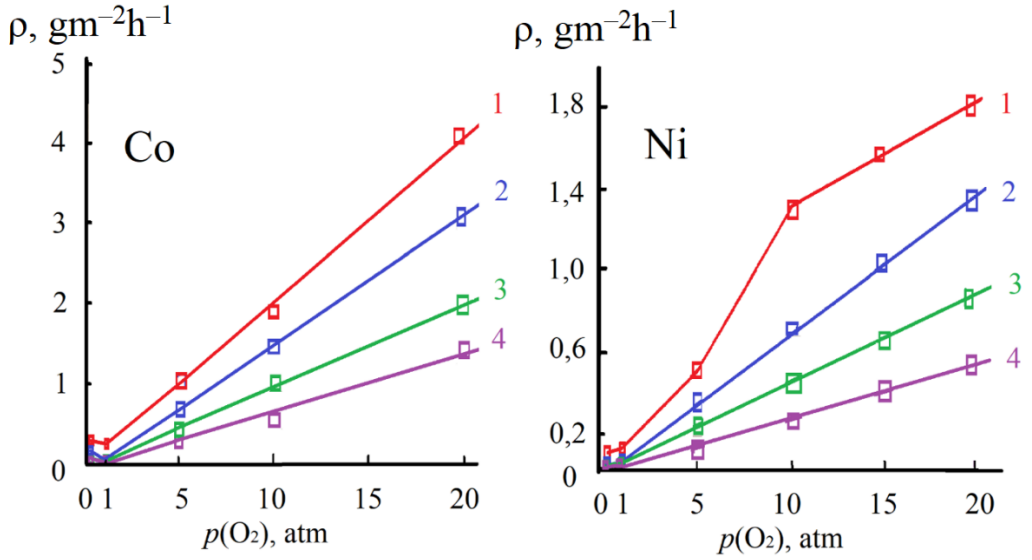

Figure 10. The influence of oxygen pressure on the corrosion rate of cobalt and nickel in 5 M HCl (1) in the presence of 1% additives: 2 – KI, 3 – octahydro-*sym*-tolyltetrazine, 4 – propargyl alcohol. t = 20°C.

With increasing molecular oxygen pressure ($p(O_2)$ to 20 atm), the corrosion rate of cobalt and nickel in 5 M HCl (t = 20°C) increases (Figure 10). The inhibitory effect for propargyl alcohol and KI decreases with increasing $p(O_2)$ [86]. Also, with an increase in $p(O_2)$, the corrosion rate of copper in HCl solutions increases, but, other things being equal, it decreases when moving from 1 M HCl to 7 M HCl (Figure 11). In 5 M HCl, as $p(O_2)$ increases, the protective effect of 1,2,3-benzotriazole on copper corrosion decreases, while that of thiourea remains virtually unchanged, which is explained by the formation of a phase film of the complex compound [87].

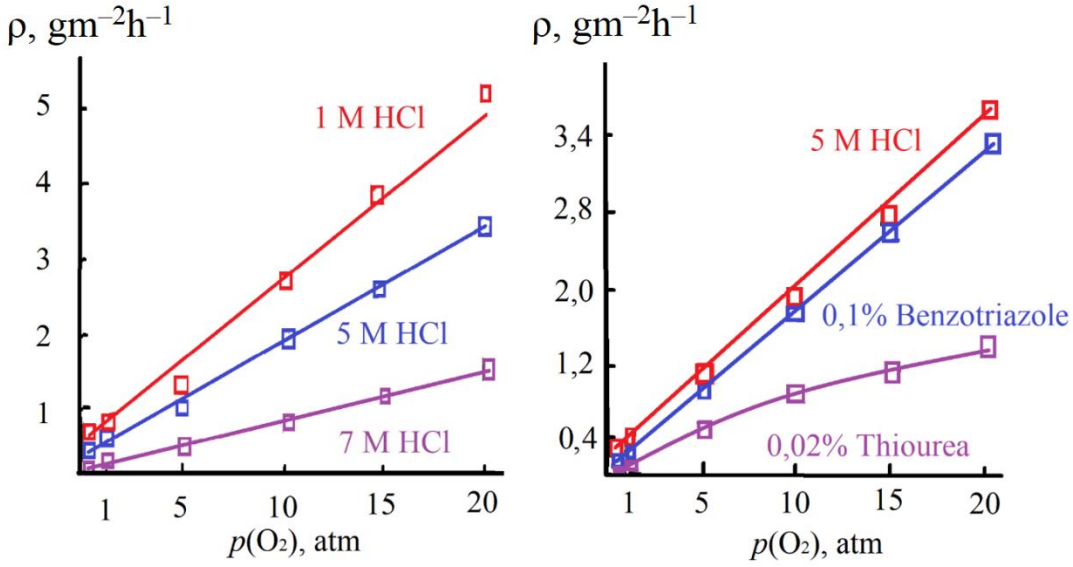

Figure 11. The influence of O_2 pressure on copper corrosion in HCl solutions. t = 20°C.

Various aspects of the inhibitory protection of copper and its base alloy with nickel (40%) in aerated solutions of HCl [88–93], H_2SO_4 [94–98] and HNO_3 [99] are considered. The kinetics of dissolved O_2 reduction and hydrogen evolution reactions on copper surface was studied in naturally aerated and air and O_2-saturated 0.5 M H_2SO_4 solutions using polarization measurements combined with the rotating disc electrode [98]. The Levich plot indicated that the dissolved O_2 reduction at the copper electrode was an apparent four-electron process. Ascorbic acid was tested as a safe inhibitor for copper corrosion in H_2SO_4 solutions at 25°C. The addition of ascorbic acid slowed down the reduction reaction of dissolved O_2 more effectively than the anodic reaction.

When studying the corrosion of copper in aerated solutions of acetic and citric acids (room *t*), the processes associated with the oxidation of the corrosion product of metallic copper – Cu(I) cations to Cu(II) cations – by dissolved O_2 were discussed [100, 101]. It was shown that effective protection of copper in the studied media is provided by the addition of substituted 1,2,4-triazole (IFKhAN-92 inhibitor). IFKhAN-92 significantly inhibits copper corrosion in aerated solutions of acetic and citric acids (up to 20 days), including the flow conditions of the corrosive medium and the presence of Cu(II) salts.

VI. Conclusion

Corrosion of a metal in an acid solution containing O_2 generally occurs as a result of its parallel reactions of interaction with the acid itself and with O_2 molecules. In acid solutions with a high content of active substance, the former reaction should predominate. In the case of metals with $E^0(Me^{z+}/Me)>0$ V, the latter is the only possible reaction.

A specific feature of corrosion occurring with oxygen depolarization is its diffusion control, which makes this process extremely sensitive to the nature of convection of the aggressive environment. In such environments, when transitioning from static conditions of metal corrosion to dynamic conditions, the rate of the process can increase significantly.

The presence of molecular oxygen in acid solutions reduces the effectiveness of metal protection with corrosion inhibitors in comparison with similar oxygen-free environments. At the same time, in inhibited environments containing O_2, the sensitivity of metal corrosion to the parameters of solution convection remains.

The nature of the effect of dissolved O_2 on metal corrosion in a formally static corrosive environment freely aerated with air is ambiguous. A good example is the corrosion of iron and its alloys. If the environment is static, then corrosion should occur exclusively through the reaction of the metal with the acid. However, the released bubbles of H_2 gas will actively stir the corrosive environment, removing diffusion restrictions on O_2 reduction. Corrosion will occur through two reactions. H_2 gas, actively released during corrosion, quickly saturates the corrosive environment, removing atmospheric oxygen from it. The only possible corrosion occurs with hydrogen depolarization. In static inhibited environments, corrosion proceeds differently. The inhibitor slows down the release of gaseous H_2, the medium is less well mixed, and dissolved O_2 is not removed from the solution. Corrosion occurs in an environment containing O_2 and with his involvement, that will impair the

protection of the metal. Unfortunately, these factors are not taken into account when interpreting the results of corrosion studies in freely aerated acid solutions.

Despite active research [16, 17, 102] in the field of acid corrosion of metals and their inhibitory protection, the role of dissolved oxygen in these processes is not taken into account in most cases, although this may be important in practice. It is necessary to search for compounds capable of effectively suppressing oxygen depolarization in acidic environments.

In our opinion, along with the search for corrosion inhibitors that suppress the absorption of hydrogen by metals [103–105], do not slow down the removal of mineral formations from metal surfaces [106], retain their effectiveness in solutions containing Fe(III) salts [8] and prevent destruction of metals under conditions of high-temperature corrosion [107–109], an urgent task of protection against acid corrosion of metals is to take into account the issues of the mechanism of the cathodic reaction of O_2 reduction discussed in this review.

References

1. M. Pourbaix and D. Zouov, Iron, *in Atlas of Electrochemical Equilibria in Aqueous Solutions*, Second English Edition, Houston: National Association of Corrosion Engineers, 1974, 307–321.
2. D. Zouov, C. Vanleugenhaghe and M. Pourbaix, Copper, *in Atlas of Electrochemical Equilibria in Aqueous Solutions*, Second English Edition, Houston: National Association of Corrosion Engineers, 1974, 385–392.
3. R.E. Huffman and N. Davidsox, Kinetics of the Ferrous Iron-Oxygen Reaction in Sulfuric Acid Solution, *J. Am. Chem. Soc*., 1956, **78**, no. 19, 4836–4842. doi: 10.1021/ja01600a004
4. M. Iwai, H. Majima and Y. Awakura, Oxidation of Fe (II) in sulfuric acid solutions with dissolved molecular oxygen, *Metall. Trans. B*, 1982, **13**, 311–318. doi: 10.1007/BF02667746
5. T. Chmielewski and W.A. Charewicz, The oxidation of Fe(II) in aqueous sulphuric acid under oxygen pressure, *Hydrometallurgy*, 1984, **12**, no. 1, 21–30. doi: 10.1016/0304-386X(84)90045-8
6. W.N. Wermink and G.F. Versteeg, The Oxidation of Fe(II) in Acidic Sulfate Solutions with Air at Elevated Pressures. Part 1. Kinetics above 1 M H_2SO_4, *Ind. Eng. Chem. Res*., 2017, **56**, no. 14, 3775–3788. doi: 10.1021/acs.iecr.6b04606
7. N. Wermink and G.F. Versteeg, The Oxidation of Fe(II) in Acidic Sulfate Solutions with Air at Elevated Pressures. Part 2. Influence of H_2SO_4 and Fe(III), *Ind. Eng. Chem. Res*., 2017, **56**, no. 14, 3789–3796. doi: 10.1021/acs.iecr.6b04641
8. Ya.G. Avdeev and Yu.I. Kuznetsov, Effect of iron(III) salts on steel corrosion in acid solutions. A review, *Int. J. Corros. Scale Inhib*., 2021, **10**, no. 3, 1069–1109. doi: 10.17675/2305-6894-2021-10-3-15

9. Ya.G. Avdeev and T.E. Andreeva, Characteristics of the Mechanism of Corrosion of Low-Carbon Steels in Acid Solutions Containing Fe(III) Salts, *Russ. J. Phys. Chem. A*, 2021, **95**, no. 6, 1128–1136. doi: 10.1134/S0036024421060029
10. Ya.G. Avdeev and T.E. Andreeva, Mechanism of Steel Corrosion in Inhibited Acid Solutions Containing Iron(III) Salts, *Russ. J. Phys. Chem. A*, 2022, **96**, no. 2, 423–434. doi: 10.1134/S0036024422020030
11. Ya.G. Avdeev, A.V. Panova and T.E. Andreeva, Role of the Convective Factor in the Corrosion of Low-Carbon Steel in Solutions of Sulfuric Acid Containing Iron(III) Sulfate, *Russ. J. Phys. Chem. A*, 2023, **97**, no. 5, 1018–1032. doi: 10.1134/S0036024423050059
12. Ya.G. Avdeev, A.V. Panova and T.E. Andreeva, Corrosion of Low-Carbon Steel in a Flow of Phosphoric Acid Solution Containing Iron(III) Phosphate, *Russ. J. Electrochem.*, 2023, **59**, no. 7, 512–523. doi: 10.1134/S1023193523070030
13. H. Kaesche, *Corrosion of metals. Physicochemical principles and current problems*, Metallurgiya, Moscow, 1984, 400 p. (in Russian).
14. K.S. Raja and D.A. Jones, Effects of dissolved oxygen on passive behavior of stainless alloys, *Corros. Sci.*, 2006, **48**, no. 7, 1623–1638. doi: 10.1016/j.corsci.2005.05.048
15. W. Forker, G. Reinhard and D. Rahner, Mechanism of the action of weak acids and their salts on the passivation of iron by oxygen, *Corros. Sci.*, 1979, **19**, no. 7, 745–751. doi: 10.1016/S0010-938X(79)80072-4
16. Ya.G. Avdeev and Yu.I. Kuznetsov, Organic Inhibitors of Metal Corrosion in Acid Solutions. I. Mechanism of Protective Action, *Russ. J. Phys. Chem.*, 2023, **97**, 413–427. doi: 10.1134/S0036024423030056
17. Ya.G. Avdeev and Yu.I. Kuznetsov, Organic Inhibitors of Metal Corrosion in Acid Solutions. II. Ways of Increasing the Protective Action and Main Groups of Compounds, *Russ. J. Phys. Chem.*, 2023, **97**, 541–549. doi: 10.1134/S0036024423040052
18. M. Finšgar and J. Jackson, Application of corrosion inhibitors for steels in acid media for the oil and gas industry: A review, *Corros. Sci.*, 2014, **86**, 17–41. doi: 10.1016/j.corsci.2014.04.044
19. T.J. Harvey, F.C. Walsh and A.H. Nahlé, A review of inhibitors for the corrosion of transition metals in aqueous acids, *J. Mol. Liq.*, 2018, **266**, 160–175. doi: 10.1016/j.molliq.2018.06.014
20. A.A. Meroufel, Corrosion Control during Acid Cleaning of Heat Exchangers, *in Corrosion and Fouling Control in Desalination Industry*, Eds.: V.S. Saji, A.A. Meroufel and A.A. Sorour, 2020, Springer, Cham., 209–224. doi: 10.1007/978-3-030-34284-5_10
21. J.A. Richardson, 2.22 - Corrosion in Hydrogen Halides and Hydrohalic Acids, *in Shreir's Corrosion*, Eds: B. Cottis, M. Graham, R. Lindsay, S. Lyon, T. Richardson, D. Scantlebury and H. Stott, 2010, Elsevier, 1207–1225. doi: 10.1016/B978-044452787-5.00197-9

22. J.A. Richardson, 2.23 - Corrosion in Sulfuric Acid, *in Shreir's Corrosion*, Eds: B. Cottis, M. Graham, R. Lindsay, S. Lyon, T. Richardson, D. Scantlebury, H. Stott, 2010, Elsevier, 1226–1249. doi: 10.1016/B978-044452787-5.00180-3
23. L. Chen, D. Lu and Y. Zhang, Organic Compounds as Corrosion Inhibitors for Carbon Steel in HCl Solution: A Comprehensive Review, *Materials*, 2022, **15**, no. 6, 2023. doi: 10.3390/ma15062023
24. V.S. Bagotskii, L.N. Nekrasov and N.A. Shumilova, Electrochemical reduction of oxygen, *Russ. Chem. Rev*., 1965, **34**, no. 10, 717–730. doi: 10.1070/RC1965v034n10ABEH001556
25. A.Sh. Groisman and N.E. Khomutov, Solubility of oxygen in electrolyte solutions, *Russ. Chem. Rev*., 1990, **59**, no. 8, 707–727. doi: 10.1070/RC1990v059n08ABEH003550
26. C.E. Boyd, Dissolved Oxygen and Redox Potential, *in Water Quality*, Springer, Boston, MA, 2000, 69–94. doi: 10.1007/978-1-4615-4485-2_5
27. N.A. Mel'nichenko, The solubility of oxygen in sea water and solutions of electrolytes according to the pulse proton NMR data, *Russ. J. Phys. Chem. A*, 2008, **82**, no. 9, 1533–1539. doi: 10.1134/S0036024408090239
28. D. Tromans, Oxygen solubility modeling in inorganic solutions: concentration, temperature and pressure effects, *Hydrometallurgy*, 1998, **50**, no. 3, 279–296. doi: 10.1016/S0304-386X(98)00060-7
29. E. Narita, F. Lawson and K.N. Han, Solubility of oxygen in aqueous electrolyte solutions, *Hydrometallurgy*, 1983, **10**, no. 1, 21–37. doi: 10.1016/0304-386X(83)90074-9
30. W. Xing, M. Yin, Q. Lv, Y. Hu, C. Liu and J. Zhang, 1 - Oxygen Solubility, Diffusion Coefficient, and Solution Viscosity, *In Rotating Electrode Methods and Oxygen Reduction Electrocatalysts*, Eds.: W. Xing, J. Zhang, G. Yin, Elsevier, 2014, 1–31. doi: 10.1016/B978-0-444-63278-4.00001-X
31. *Chemist's Handbook. Vol. 3. Chemical equilibrium and kinetics. Properties of solutions. Electrode processes*., Eds.: B.P. Nikolsky, O.N. Grigorov, M.E. Pozin, B.A. Paray-Koshits, V.A. Rabinovich, P.G. Romankov and D.A. Friedrichsberg, 1964, Chemistry, Moscow, Leningrad, 715–725 (in Russian).
32. W. Caia, X. Zhaoa, C. Liub, W. Xinga and J. Zhang, 2 – Electrode Kinetics of Electron-Transfer Reaction and Reactant Transport in Electrolyte Solution, *In Rotating Electrode Methods and Oxygen Reduction Electrocatalysts*, Eds.: W. Xing, J. Zhang, G. Yin, Elsevier, 2014, 33–65. doi: 10.1016/B978-0-444-63278-4.00002-1
33. L. Feng, X. Sun, S. Yao, C. Liu, W. Xing and J. Zhang, 3 – Electrocatalysts and Catalyst Layers for Oxygen Reduction Reaction, *In Rotating Electrode Methods and Oxygen Reduction Electrocatalysts*, Eds.: W. Xing, J. Zhang, G. Yin, Elsevier, 2014, 67–132. doi: 10.1016/B978-0-444-63278-4.00003-3
34. F. Si, Y. Zhang, L. Yan, J. Zhu, M. Xiao, C. Liu, W. Xing and J. Zhang, 4 – Electrochemical Oxygen Reduction Reaction, *In Rotating Electrode Methods and Oxygen Reduction Electrocatalysts*, Eds.: W. Xing, J. Zhang, G. Yin, Elsevier, 2014, 133–170. doi: 10.1016/B978-0-444-63278-4.00004-5

35. C. Du, Q. Tan, G. Yin and J. Zhang, 5 – Rotating Disk Electrode Method, *In Rotating Electrode Methods and Oxygen Reduction Electrocatalysts*, Eds.: W. Xing, J. Zhang, G. Yin, Elsevier, 2014, 171–198. doi: 10.1016/B978-0-444-63278-4.00005-7
36. Z. Jia, G. Yin and J. Zhang, 6 – Rotating Ring-Disk Electrode Method, *In Rotating Electrode Methods and Oxygen Reduction Electrocatalysts* Eds.: W. Xing, J. Zhang, G. Yin, Elsevier, 2014, 199–229. doi: 10.1016/B978-0-444-63278-4.00006-9
37. C. Du, Y. Sun, T. Shen, G. Yin and J. Zhang, 7 – Applications of RDE and RRDE Methods in Oxygen Reduction Reaction, *In Rotating Electrode Methods and Oxygen Reduction Electrocatalysts*, Eds.: W. Xing, J. Zhang, G. Yin, Elsevier, 2014, 231–277. doi: 10.1016/B978-0-444-63278-4.00007-0
38. X. Wang, Z. Li, Y. Qu, T. Yuan, W. Wang, Y. Wu and Y. Li, Review of Metal Catalysts for Oxygen Reduction Reaction: From Nanoscale Engineering to Atomic Design, *Chem*, 2019, **5**, no. 6, 1486–1511. doi: 10.1016/j.chempr.2019.03.002
39. I. Dumitrescu and R.M. Crooks, Effect of mass transfer on the oxygen reduction reaction catalyzed by platinum dendrimer encapsulated nanoparticles, *PNAS*, 2012, **109**, no. 29, 11493–11497. doi: 10.1073/pnas.1201370109
40. S. Chen and A. Kucernak, Electrocatalysis under Conditions of High Mass Transport Rate: Oxygen Reduction on Single Submicrometer-Sized Pt Particles Supported on Carbon, *J. Phys. Chem. B*, 2004, **108**, no. 10, 3262–3276. doi: 10.1021/jp036831j
41. A.L. Colley, J.V. Macpherson and P.R. Unwin, Effect of high rates of mass transport on oxygen reduction at copper electrodes: Implications for aluminium corrosion, *Electrochem. Commun.*, 2008, **10**, no. 9, 1334–1336. doi: 10.1016/j.elecom.2008.06.032
42. D. Pletcher and S. Sotiropoulos, A study of cathodic oxygen reduction at platinum using microelectrodes, *J. Electroanal. Chem.*, 1993, **356**, no. 1–2, 109–119. doi: 10.1016/0022-0728(93)80514-I
43. M. Stratmann and J. Müller, The mechanism of the oxygen reduction on rust-covered metal substrates, *Corros. Sci.*, 1994, **36**, no. 2, 327–359. doi: 10.1016/0010-938X(94)90161-9
44. H.S. Wroblowa, Y.-C. Pan and G. Razumney, Electroreduction of oxygen: A new mechanistic criterion, *J. Electroanal. Chem. Interfacial Electrochem.*, 1976, **69**, no. 2, 195–201. doi: 10.1016/S0022-0728(76)80250-1
45. C. Song and J. Zhang, Electrocatalytic Oxygen Reduction Reaction, *In: PEM Fuel Cell Electrocatalysts and Catalyst Layers*, Ed.: J. Zhang, 2008, Springer, London, 89–134. doi: 10.1007/978-1-84800-936-3_2
46. L. Khotseng, Oxygen Reduction Reaction, *In: Electrocatalysts for Fuel Cells and Hydrogen Evolution - Theory to Design*, Eds.: A. Ray, I. Mukhopadhyay and R.K. Pati, 2018, IntechOpen. doi: 10.5772/intechopen.79098
47. N.M. Marković and P.N. Ross, Surface science studies of model fuel cell electrocatalysts, *Surf. Sci. Rep.*, 2002, **45**, no. 4–6, 117–229. doi: 10.1016/S0167-5729(01)00022-X

48. *Electrochemical Oxygen Reduction. Fundamental and Applications*, Ed.: P.K. Shen, 2021, Springer Singapore, 254 p. doi: 10.1007/978-981-33-6077-8
49. L. Vracar, Oxygen Reduction Reaction in Acid Solution. *In: Encyclopedia of Applied Electrochemistry*. Eds.: G. Kreysa, K. Ota and R.F. Savinell, 2014, Springer, New York, 1485–1491. doi: 10.1007/978-1-4419-6996-5_481
50. R. Haider, X. Yuan, and M. Bilal, Oxygen Reduction Reaction. *In: Methods for Electrocatalysis*, Eds.: Inamuddin, R. Boddula and A. Asiri, 2020, Springer, Cham., 375–400. doi: 10.1007/978-3-030-27161-9_15
51. A.I. Danilov, E.B. Molodkina and Y.M. Polukarov, Surface and Subsurface Oxygen on Platinum in a 0.5 M H_2SO_4 Solution, *Russ. J. Electrochem*., 2004, **40**, 585–596. doi: 10.1023/B:RUEL.0000032007.83996.27
52. A.I. Danilov, E.B. Molodkina and Y.M. Polukarov, Surface and Subsurface Oxygen on Platinum in a 0.5 M H_2SO_4 + 0.01 M $CuSO_4$ Solution, *Russ. J. Electrochem*., 2004, **40**, 597–603. doi: 10.1023/B:RUEL.0000032008.20535.12
53. D.V. Savinova, E.B. Molodkina, A.I. Danilov and Y.M. Polukarov, Surface and Subsurface Oxygen on Platinum in a Perchloric Acid Solution, *Russ. J. Electrochem*., 2004, **40**, 683–687. doi: 10.1023/B:RUEL.0000035248.39620.f7
54. D.V. Savinova, E.B. Molodkina, A.I. Danilov and Y.M. Polukarov, Surface and Subsurface Oxygen on Platinum in a Copper Perchlorate Solution, *Russ. J. Electrochem*., 2004, **40**, 687–694. doi: 10.1023/B:RUEL.0000035249.80348.77
55. V.M. Andoralov, M.R. Tarasevich and O.V. Tripachev, Oxygen reduction reaction on polycrystalline gold. Pathways of hydrogen peroxide transformation in the acidic medium, *Russ. J. Electrochem*., 2011, **47**, no. 12, 1327–1336. doi: 10.1134/S1023193511120020
56. D.H. Evans and J.J. Lingane, The chronopotentiometric reduction of oxygen at gold electrodes, *J. Electroanal. Chem*., 1963, **6**, no. 4, 283–299. doi: 10.1016/0022-0728(63)80107-2
57. J.J. Lingane, Chronopotentiometric study of oxygen reduction at a platinum wire cathode, *J. Electroanal. Chem*., 1961, **2**, no. 4, 296–309. doi: 10.1016/0022-0728(61)85003-1
58. L. Zhang, C. Song, J. Zhang, H. Wang and D.P. Wilkinson, Temperature and pH Dependence of Oxygen Reduction Catalyzed by Iron Fluoroporphyrin Adsorbed on a Graphite Electrode, *J. Electrochem. Soc*., 2005, **152**, A2421. doi: 10.1149/1.2109667
59. K. Lee, L. Zhang, H. Lui, R. Hui, Z. Shi and J. Zhang, Oxygen reduction reaction (ORR) catalyzed by carbon-supported cobalt polypyrrole (Co-PPy/C) electrocatalysts, *Electrochim. Acta*, 2009, **54**, no. 20, 4704–4711. doi: 10.1016/j.electacta.2009.03.081
60. J.X. Wang, N.M. Markovic and R.R. Adzic, Kinetic Analysis of Oxygen Reduction on Pt(111) in Acid Solutions: Intrinsic Kinetic Parameters and Anion Adsorption Effects, *J. Phys. Chem. B*, 2004, **108**, no. 13, 4127–4133. doi: 10.1021/jp037593v

61. I. Srejić, M. Smiljanić, Z. Rakočević and S. Štrbac, Oxygen Reduction on Polycrystalline Pt and Au Electrodes in Perchloric Acid Solution in the Presence of Acetonitrile, *Int. J. Electrochem. Sci*., 2011, **6**, no. 8, 3344–3354. doi: 10.1016/S1452-3981(23)18256-3
62. L.I. Antropov, E.M. Makushin and V.F. Panasenko, *Ingibitory korrozii metallov (Metal Corrosion Inhibitors)*, Tehnika, Kiev, 1981, 183 p. (in Russian).
63. E.S. Bulavina, N.I. Podobaev and V.I. Rodionova, The influence of movement speed and temperature on the corrosion of low-carbon steel with and without scale in a 4% hydrochloric acid solution deaerated with hydrogen and saturated with oxygen, *Ingibitory korrozii metallov (Metal Corrosion Inhibitors)*, Eds.: S.A. Balezin, F.B. Glikina, N.I. Podobaev, N.G. Klyuchnikov and E.G. Zak, Moscow, MGPI im. V.I. Lenina, 1969, 123–128 (in Russian).
64. Ya.G. Avdeev and T.E. Andreeva, Mechanism of Corrosion of Low-Carbon Steel in 1 M Solutions of Hydrochloric Acid Saturated with Oxygen, *Russ. J. Phys. Chem. A*, 2022, **96**, no. 10, 2189–2197. doi: 10.1134/S0036024422100041
65. Q. Zhang, P. Liu, Z. Zhu, Z. Ye, J. Zhang, F. Cao and X. Li, Quantitative analysis of the polarization behavior of iron in an aerated acidic solution using SECM, *Electrochem. Commun*., 2018, **93**, 143–147. doi: 10.1016/j.elecom.2018.07.007
66. J.A. Tamayo-Sepúlveda, F.A. Vásquez-Arroyave and J.A. Calderón-Gutiérrez, Effect of aeration on Tafelian behavior of the carbon steel corrosion in acid sulfate medium, *Rev. Fac. Ing*., 2017, no. 83, 36–42. doi: 10.17533/udea.redin.n83a05
67. Y. Lu, H. Xu, J. Wang and X. Kong, Oxygen reduction mechanism on copper in a 0.5 M H_2SO_4, *Electrochim. Acta*, 2009, **54**, no. 15, 3972–3978. doi: 10.1016/j.electacta.2009.02.019
68. B.Ya. Konyaev, *Study of the process of oxygen depolarization during corrosion of nickel in sulfuric acid solutions under various hydrodynamic conditions. Autoabstract of the dissertation of Ph.D. in Chemistry*, MGPI im. V.I. Lenina, Moscow, 1974, 25 p. (in Russian).
69. A.I. Molodov, *Formation of low-valent particles and their role in multi-electron processes of metal discharge-ionization. Autoabstract of the dissertation of D.Sci. in Chemistry*, Karpov Institute of Physical Chemistry, Moscow, 1988. 44 p. (in Russian).
70. Z.A. Foroulis and H.H. Uhlig, Effect of Velocity and Oxygen on Corrosion of Iron in Sulfuric Acid, *J. Electrochem. Soc*., 1964, **111**, 13–17. doi: 10.1149/1.2426050
71. H. Bala, Electrochemical investigation of corrosion of iron in oxygen saturated sulphuric acid solutions, *Br. Corros. J*., 1988, **23**, no. 1, 29–36. doi: 10.1179/000705988798271135
72. J. Postlethwaite and D.R. Hurp, Some effects of flow and aeration on the corrosion behaviour of nickel in sulphuric acid solutions, *Corros. Sci*., 1967, **7**, no. 7, 435–445. doi: 10.1016/S0010-938X(67)80056-8
73. W.G. Whitman and R.P. Russell, The Acid Corrosion of Metals. Effect of Oxygen and Velocity, *Ind. Eng. Chem*., 1925, **17**, no. 4, 348–354. doi: 10.1021/ie50184a008

74. L. Burzyńska, A. Maraszewska and Z. Zembura, The corrosion of Cu-47.3 at% Zn BRASS in aerated 1.0 M HCl, *Corros. Sci*., 1996, **38**, no. 2, 337–347. doi: 10.1016/0010-938X(96)00132-1
75. Y. Che, Z. Han, B. Luo, D. Xia, J. Shi, Z. Gao and J. Wang, Corrosion Mechanism Differences of Tinplate in Aerated and Deaerated Citric Acid Solution, *Int. J. Electrochem. Sci*., 2012, **7**, no. 10, 9997–10007. doi: 10.1016/S1452-3981(23)16253-5
76. L.I. Antropov and I.S. Pogrebova, Relationship between the adsorption of organic compounds and their effect on the corrosion of metals in acidic environments, *Corrosion and Corrosion Protection, Vol. 2: Part of Results of Science and Technology Series*, VINITI, Moscow, 1973, 27–112 (in Russian).
77. N.I. Podobaev, The role of oxygen in steel corrosion in acids in the presence of inhibitors, *Ingibitory korrozii metallov (Metal corrosion inhibitors)*, Ed.: S.A. Balezin, Publishing House "Sudostroyeniye", Moscow, 1965, 59–64 (in Russian).
78. S.A. Balezin, F.B. Glikina and R.V. Frolova, The effect of hydrazine on the corrosion of steel 20 in dilute solutions of hydrochloric and sulfuric acids at a temperature of 100°C, *Ingibitory korrozii metallov (Metal corrosion inhibitors)*, Ed.: S.A. Balezin, Publishing House "Sudostroyeniye", Moscow, 1965, 72–79 (in Russian).
79. S.A. Balezin, V.I. Rodionova and L.Z. Bondarenko, Corrosion rate of alloy steels in circulating hydrochloric acid solutions, *Ingibitory korrozii metallov (Metal Corrosion Inhibitors)*, Eds.: S.A. Balezin, F.B. Glikina, N.I. Podobaev, N.G. Klyuchnikov and E.G. Zak, Moscow, MGPI im. V.I. Lenina, 1969, 101–108 (in Russian).
80. Ya.G. Avdeev and K.L. Anfilov, Effect of dissolved oxygen on the electrode reactions of low-carbon steel in 1 M HCl containing butyndiol and propargyl alcohol, *Int. J. Corros. Scale Inhib*., 2023, **12**, no. 1, 84–100. doi: 10.17675/2305-6894-2023-12-1-5
81. N.I. Podobaev and V.I. Kotov, The influence of oxygen on the adsorption of acid corrosion inhibitors on iron, *Ingibitory korrozii metallov (Metal Corrosion Inhibitors)*, Eds.: S.A. Balezin, F.B. Glikina, N.I. Podobaev, N.G. Klyuchnikov and E.G. Zak, Moscow, MGPI im. V.I. Lenina, 1969, 24–29 (in Russian).
82. B.O. Hasan and S.A. Sadek, The effect of temperature and hydrodynamics on carbon steel corrosion and its inhibition in oxygenated acid–salt solution, *J. Ind. Eng. Chem*., 2014, **20**, no. 1, 297–307. doi: 10.1016/j.jiec.2013.03.034
83. M.S. Morad, An electrochemical study on the inhibiting action of some organic phosphonium compounds on the corrosion of mild steel in aerated acid solutions, *Corros. Sci*., 2000, **42**, no. 8, 1307–1326. doi: 10.1016/S0010-938X(99)00138-9
84. R.J. Meakins, Effect of Atmospheric Oxygen on the Electrode Potential and Corrosion Inhibition of Steel in Acid Solutions, *Br. Corros. J*., 1971, **6**, no. 3, 109–110. doi: 10.1179/000705971798323955
85. A.Y. Musa, A.A.H. Kadhum and A.B. Muhamad, Corrosion Inhibitor Film Forming in Aerated and Deaerated Solutions, *Int. J. Electrochem. Sci*., 2010, **5**, no. 12, 1911–1921. doi: 10.1016/S1452-3981(23)15394-6

86. T.I. Kurilovich and N.G. Klyuchnikov, The influence of oxygen and nitrogen pressure on the corrosion of cobalt and nickel in hydrochloric acid, *Ingibitory korrozii metallov (Metal Corrosion Inhibitors)*, Eds.: S.A. Balezin, E.G. Zak, F.B. Glikina, N.I. Podobaev and N.G. Klyuchnikov, Moscow, MGPI im. V.I. Lenina, 1972, 172–181 (in Russian).
87. T.I. Kurilovich and N.G. Klyuchnikov, Corrosion behavior of copper in hydrochloric acid under oxygen pressure, *Ingibitory korrozii metallov (Metal Corrosion Inhibitors)*, Eds.: S.A. Balezin, E.G. Zak, F.B. Glikina, N.I. Podobaev and N.G. Klyuchnikov, Moscow, MGPI im. V.I. Lenina, 1972, 168–172 (in Russian).
88. K.F. Khaled and N. Hackerman, Ortho-substituted anilines to inhibit copper corrosion in aerated 0.5 M hydrochloric acid, *Electrochim. Acta*, 2004, **49**, no. 3, 485–495. doi: 10.1016/j.electacta.2003.09.005
89. E.M. Sherif and S.-M. Park, Effects of 2-amino-5-ethylthio-1,3,4-thiadiazole on copper corrosion as a corrosion inhibitor in aerated acidic pickling solutions, *Electrochim. Acta*, 2006, **51**, no. 28, 6556–6562. doi: 10.1016/j.electacta.2006.04.047
90. E.M. Sherif, R.M. Erasmus and J.D. Comins, Corrosion of copper in aerated acidic pickling solutions and its inhibition by 3-amino-1,2,4-triazole-5-thiol, *J. Colloid Interface Sci.*, 2007, **306**, no. 1, 96–104. doi: 10.1016/j.jcis.2006.10.029
91. D.-Q. Zhang, L.-X. Gao and G.-D. Zhou, Inhibition of copper corrosion in aerated hydrochloric acid solution by heterocyclic compounds containing a mercapto group, *Corros. Sci.*, 2004, **46**, no. 12, 3031–3040. doi: 10.1016/j.corsci.2004.04.012
92. D.-Q. Zhang, Q.-R. Cai, L.-X. Gao and K.Y. Lee, Effect of serine, threonine and glutamic acid on the corrosion of copper in aerated hydrochloric acid solution, *Corros. Sci.*, 2008, **50**, no. 12, 3615–3621. doi: 10.1016/j.corsci.2008.09.007
93. E.M. Sherif and S.-M. Park, Inhibition of copper corrosion in acidic pickling solutions by N-phenyl-1,4-phenylenediamine, *Electrochim. Acta*, 2006, **51**, no. 22, 4665–4673. doi: 10.1016/j.electacta.2006.01.007
94. G. Moretti and F. Guidi, Tryptophan as copper corrosion inhibitor in 0.5 M aerated sulfuric acid, *Corros. Sci.*, 2002, **44**, no. 9, 1995–2011. doi: 10.1016/S0010-938X(02)00020-3
95. G. Quartarone, T. Bellomi and A. Zingales, Inhibition of copper corrosion by isatin in aerated 0.5 M H_2SO_4, *Corros. Sci.*, 2003, **45**, no. 4, 715–733. doi: 10.1016/S0010-938X(02)00134-8
96. H. Saifi, M.C. Bernard, S. Joiret, K. Rahmouni, H. Takenouti and B. Talhi, Corrosion inhibitive action of cysteine on Cu–30Ni alloy in aerated 0.5M H_2SO_4, *Mater. Chem. Phys.*, 2010, **120**, no. 2–3, 661–669. doi: 10.1016/j.matchemphys.2009.12.011
97. D.-Q. Zhang, L.-X. Gao and G.-D. Zhou, Inhibition of copper corrosion by bis-(1,1′-benzotriazoly)-α,ω-diamide compounds in aerated sulfuric acid solution, *Appl. Surf. Sci.*, 2006, **252**, no. 14, 4975–4981. doi: 10.1016/j.apsusc.2005.07.010
98. M.A. Amin, Role of dissolved oxygen reduction in improvement inhibition performance of ascorbic acid during copper corrosion in 0.50mol/L sulphuric acid, *Chin. Chem. Lett.*, 2010, **21**, no. 3, 341–345. doi: 10.1016/j.cclet.2009.10.026

99. A. Zarrouk, H. Zarrok, R. Salghi, B. Hammouti, E.E. Ebenso, F. Bentiss, H. Oudda, M. Elbakri and R. Touir, Inhibition of Copper Corrosion by 2-Aminobenzenethiol in Aerated 2 M HNO_3 Medium, *Int. J. Electrochem. Sci*., 2013, **8**, no. 9, 11000–11018. doi: 10.1016/S1452-3981(23)13165-8
100. Ya.G. Avdeev, K.L. Anfilov, E.P. Rukhlenko and Yu.I. Kuznetsov, Inhibitory protection of copper in acetic acid solutions, *Int. J. Corros. Scale Inhib*., 2021, **10**, no. 1, 302–313. doi: 10.17675/2305-6894-2020-10-1-17
101. Ya.G. Avdeev, K.L. Anfilov, E.P. Rukhlenko and Yu.I. Kuznetsov, Inhibitor protection of copper in citric acid solutions, *Int. J. Corros. Scale Inhib*., 2021, **10**, no. 3, 911–923. doi: 10.17675/2305-6894-2021-10-3-5
102. Ya.G. Avdeev and Yu.I. Kuznetsov, Acid corrosion of metals and its inhibition. A critical review of the current problem state, *Int. J. Corros. Scale Inhib*., 2022, **11**, no. 1, 111–141. doi: 10.17675/2305-6894-2022-11-1-6
103. Ya.G. Avdeev, T.A. Nenasheva, A.Yu. Luchkin, A.I. Marshakov and Yu.I. Kuznetsov, Effect of Quaternary Ammonium Salts and 1,2,4-Triazole Derivatives on Hydrogen Absorption by Mild Steel in Hydrochloric Acid Solution, *Materials*, 2022, **15**, no. 19, 6989. doi: 10.3390/ma15196989
104. Ya.G. Avdeev, T.A. Nenasheva, A.Yu. Luchkin, A.I. Marshakov and Yu.I. Kuznetsov, Thin 1,2,4-Triazole Films for the Inhibition of Carbon Steel Corrosion in Sulfuric Acid Solution, *Coatings*, 2023, **13**, no. 7, 1221. doi: 10.3390/coatings13071221
105. Ya.G. Avdeev, T.A. Nenasheva, A.Yu. Luchkin, A.I. Marshakov and Yu.I. Kuznetsov, Thin Films of a Complex Polymer Compound for the Inhibition of Iron Alloy Corrosion in a H_3PO_4 Solution, *Polymers*, 2023, **15**, no. 21, 4280. doi: 10.3390/polym15214280
106. Ya.G. Avdeev and Yu.I. Kuznetsov, Iron oxide and oxyhydroxide phases formed on steel surfaces and their dissolution in acid media. Review, *Int. J. Corros. Scale Inhib*., 2023, **12**, no. 2, 366–409. doi: 10.17675/2305-6894-2023-12-2-1
107. Ya.G. Avdeev, Yu.I. Kuznetsov, Inhibitory protection of steels from high-temperature corrosion in acid solutions. A review. Part 1, *Int. J. Corros. Scale Inhib*., 2020, **9**, no. 2, 394–426. doi: 10.17675/2305-6894-2020-9-2-2
108. Ya.G. Avdeev and Yu.I. Kuznetsov, Inhibitory protection of steels from high-temperature corrosion in acid solutions. A review. Part 2., *Int. J. Corros. Scale Inhib*., 2020, **9**, no. 3, 867–902. doi: 10.17675/2305-6894-2020-9-3-5
109. Ya.G. Avdeev and Yu.I. Kuznetsov, Inhibitory protection of steels in acid solutions under high-temperature corrosion conditions. A review. Part 3, *Int. J. Corros. Scale Inhib*., 2020, **9**, no. 4, 1194–1236. doi: 10.17675/2305-6894-2020-9-4-3

♦ ♦ ♦